

Supplementary Information

Nonequilibrium switching of segmental states can influence compaction of chromatin

Soudamini Sahoo^{1,2}, Sangram Kadam³, Ranjith Padinhateeri^{3,*}, and P. B. Sunil Kumar^{1,4,5,†}

¹*Department of Physics, Indian Institute of Technology Palakkad, Palakkad, 678623, India*

²*Department of Physics and Astronomy, National Institute of Technology Rourkela, Rourkela, 769008, India*

³*Department of Biosciences and Bioengineering, Indian Institute of Technology Bombay, Powai, Mumbai, 400076, India*

⁴*Department of Physics, Indian Institute of Technology Madras, Chennai, 600036, India*

⁵*Center for Soft and Biological Matter, Indian Institute of Technology Madras, Chennai, 600036, India*

Corresponding authors: * ranjithp@iitb.ac.in, † sunil@iitm.ac.in

This PDF file includes:

Supporting Text

Figures S1 to S4

Legends for Movie S1

Other supporting materials for this manuscript include the following:

Movie S1

S1 Probability Current and Kolmogorov condition

To analyse the nonequilibrium nature of the model, we will represent each segment to be in one of the four discrete states, represented by 1) phobic extended, 2) phobic collapsed, 3) phobic collapsed, and 4) phobic collapsed. The populations of segments in these four states are represented by N_1, N_2, N_3 , and N_4 , respectively. The probability for a segment to be in any of these states is then given by $P_i = \frac{N_i}{N}$. Here, N_i and P_i satisfy,

$$N_1 + N_2 + N_3 + N_4 = N, \quad (\text{S1})$$

$$P_1 + P_2 + P_3 + P_4 = 1. \quad (\text{S2})$$

The states and the associated transition rates are marked in the figure S1.

The associated currents are given by,

$$\begin{aligned} J_1 &= P_1 k_{12} - P_2 k_{21}, \\ J_2 &= P_2 k_{23} - P_3 k_{32}, \\ J_3 &= P_3 k_{34} - P_4 k_{43}, \\ J_4 &= P_4 k_{41} - P_1 k_{14}. \end{aligned} \quad (\text{S3})$$

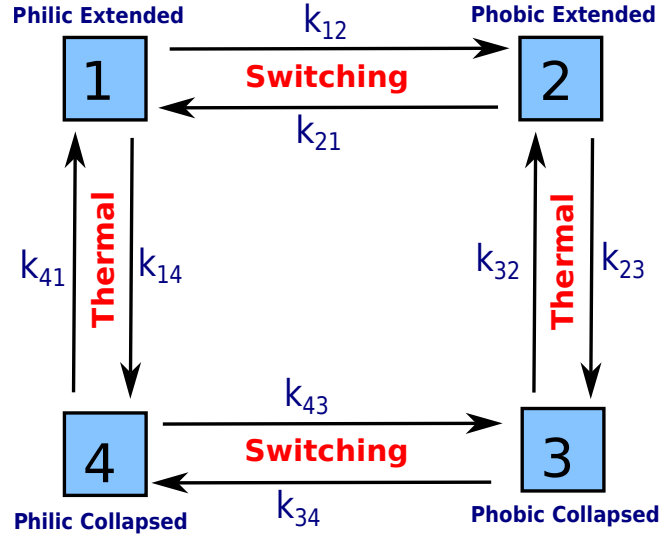


FIG. S1: Conformations of chromatin segments represented as a four-state system with corresponding transition rates.

The rate of change of populations in each state is given by the difference in current flowing in and out of the state, and is given by,

$$\begin{aligned}\frac{dP_1}{dt} &= J_4 - J_1, \\ \frac{dP_2}{dt} &= J_1 - J_2, \\ \frac{dP_3}{dt} &= J_2 - J_3, \\ \frac{dP_4}{dt} &= J_3 - J_4.\end{aligned}$$

At steady state $\frac{dP_i}{dt} = 0$, where $i = 1, 2, 3$, and $4 \Rightarrow J_4 = J_1$, $J_1 = J_2$, $J_2 = J_3$, and $J_3 = J_4$. This steady state condition along with S3 and S2 leads to the following matrix equation,

$$\begin{bmatrix} (k_{12} + k_{14} + k_{41}) & -(k_{21} - k_{41}) & k_{41} \\ k_{12} & -(k_{21} + k_{23}) & k_{32} \\ -k_{43} & (k_{23} - k_{43}) & -(k_{32} + k_{34} + k_{43}) \end{bmatrix} \begin{bmatrix} P_1 \\ P_2 \\ P_3 \end{bmatrix} = \begin{bmatrix} k_{41} \\ 0 \\ -k_{43} \end{bmatrix} \quad (\text{S4})$$

$$\text{Or } KP = M \quad (\text{S5})$$

from which we can get the expressions for the P_i s, in terms of the rates, as,

$$\begin{aligned}|K|P_1 &= k_{41}k_{21}(k_{32} + k_{34}) + k_{41}k_{23}k_{34} + k_{43}k_{32}k_{21}, \\ |K|P_2 &= k_{41}k_{12}(k_{32} + k_{34}) + k_{43}k_{32}(k_{12} + k_{14}), \\ |K|P_3 &= k_{41}k_{12}(k_{23} + k_{43}) + k_{43}k_{23}(k_{12} + k_{14}),\end{aligned} \quad (\text{S6})$$

where, $|K|$ is the determinant of the matrix $[K]$. Using S6 we can get an expression for the current in the loop J_1 as,

$$\begin{aligned}J_1 &= P_1k_{12} - P_2k_{21} \\ &= (k_{12}k_{23}k_{34}k_{41} - k_{14}k_{43}k_{32}k_{21})/|K|.\end{aligned} \quad (\text{S7})$$

The thermally activated transition rate from an extended phobic to collapsed phobic is much higher than that from collapsed phobic to extended phobic, i.e $k_{32} \ll k_{23}$. Similarly the rate of transition from a collapsed philic to extended philic is much higher than that from extended philic to collapsed philic, i.e $k_{14} \ll k_{41}$. Since in the present work all other rates are taken as equal and constant, this current is nonzero at steady state. At equilibrium the current should be zero which leads us to the Kolmogorov condition for equilibrium as,

$$k_{12}k_{23}k_{34}k_{41} = k_{14}k_{43}k_{32}k_{21}. \quad (\text{S8})$$

S2 Steady state parameters

Equations 3 and 4, which are reproduced below for convenience,

$$R_{\pm} = \frac{N_s R_f}{\eta + \exp(\mu[N_- - N_+ - A_0])}, \quad (\text{S9})$$

$$R_{\mp} = \frac{N_s R_f}{1 + \exp(-\mu[N_- - N_+ - A_0])}, \quad (\text{S10})$$

are constitutive equations that relate the rate of active switching process to the steady state fraction of philic and phobic states.

At any instant of Monte Carlo step, the fraction of philic segments is $\frac{N_+}{N_s}$ and that of phobic segments is $\frac{N_-}{N_s}$. At steady state, the rate of transition from the philic to phobic segments is equal to that of phobic to philic. Also, at steady state, N_+ approaches N_+^0 and N_- approaches N_-^0 i.e. the steady-state should also obey $\langle N_- \rangle - \langle N_+ \rangle = A_0$. Hence,

$$\begin{aligned} \frac{N_+}{N_s} \times R_{\pm} &= \frac{N_-}{N_s} \times R_{\mp} \\ \Rightarrow \frac{N_+^0}{N_s} \times R_{\pm} &= \frac{N_-^0}{N_s} \times R_{\mp} \\ \Rightarrow \eta &= 2 \frac{N_+^0}{N_-^0} - 1. \end{aligned} \quad (\text{S11})$$

In our case, we choose $A_0 = 0$ and set $\eta = 1$. μ controls the fluctuation of $|N_+ - N_-|$, which can be thought of as a measure of the availability of active agents and other factors that are responsible for the switching, and the height of the barrier.

S3 Comparison of Monte Carlo time with biological time scale

One Monte Carlo Step is when, on average, all beads are attempted to move once. We have defined the polymer and segment relaxation times in units of that. From experiments, it is seen that the relaxation time of chromatin of length 50kb is approximately 150 seconds [1]. Comparing this with the relaxation time of our polymer of 1024 beads, which is equivalent to 256 nucleosomes, we can estimate 1 MCS as approximately 0.1 ms. In these units, the switching time scale used in the simulation ranges from 0.1 ms to 250 minutes. The known assembly/disassembly time [2] of a nucleosome is of the order of one minute, which is close to the relaxation time of the polymer in our simulation. In principle, it should be possible to vary the assembly/disassembly time of the nucleosome by varying the concentration of the enzymes and to explore experimentally the range of time scales that we have simulated.

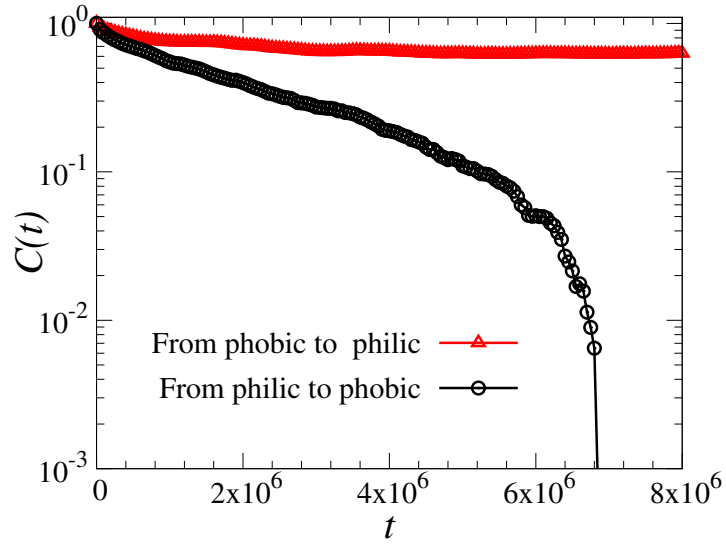


FIG. S2: Relaxation of unit end to end vector of a polymer of length 512 when switched from phobic to philic and vice versa.

S4 Asymmetry in relaxation time of philic and phobic states

In the simulations reported here, the transition rates from phobic to philic and vice versa are the same. However, there is considerable asymmetry in the relaxation time of the segments depending on whether they are switched from phobic or philic state. We check this by calculating the auto-correlation $C(t)$ of the unit end to end vector of a homogeneous polymer of length 512, when switched from the equilibrated phobic/philic state to the philic/phobic state. This is shown in Fig. S2. It is clear from the figure that the relaxation is considerably faster when switch from philic to phobic state.

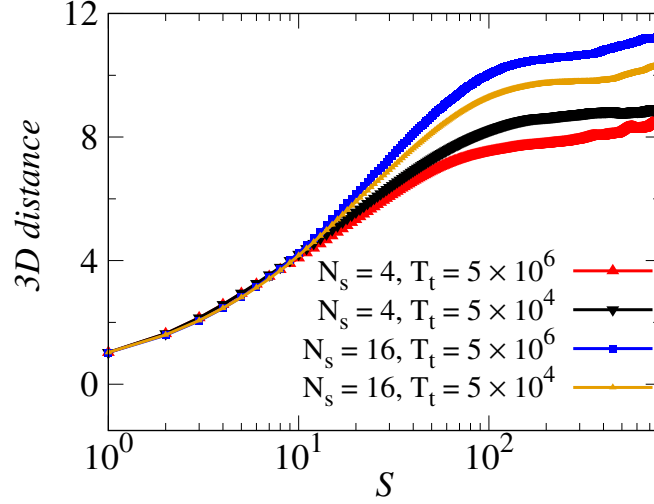


FIG. S3: Average 3D distance between pairs of beads of the polymer separated by genomic distance S for different combinations of N_s and T_t values.

S5 Spatial distance matrix

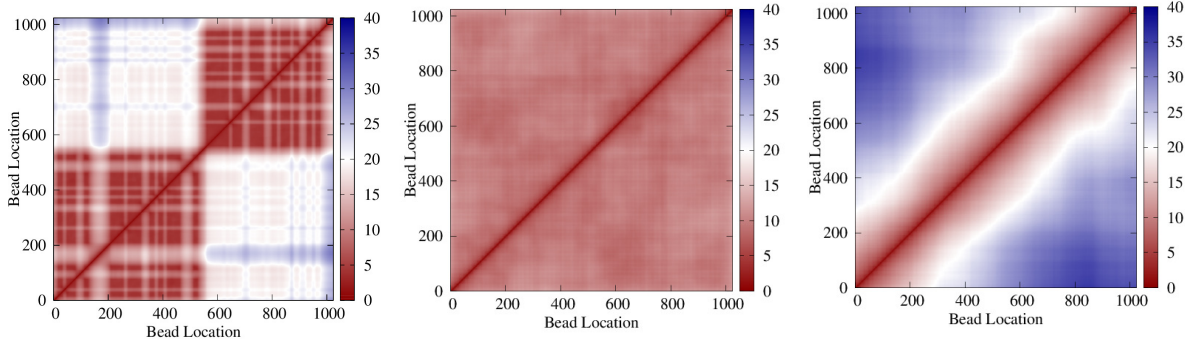


FIG. S4: Spatial distance matrix — 3D distance between all bead pairs between i and j — for a copolymer with solvo-phobic and solvo-philic segments of size $N_s = 16$. (a) Passive polymer with segments distributed randomly, (b) polymer with slow switching of the segmental states ($T_t \approx \tau_p$), and (c) polymer with fast switching ($T_t \approx \tau_s$). These plots are for a single realisation averaged over time.

Figure S4 shows the spatial distance matrix for different switching times. For a passive polymer (see Fig. S4(a)), we see two TAD-like structures (domains) arising due to two compact clusters trapped in long-lived meta-stable states. Please note that these plots are generated from one realization after averaging over many steady-state time observations. Since there are no boundary-determining factors, the location of the boundary and size of the domains may vary in different realizations. In Fig. S4(b), where the polymer switching time is comparable to the polymer relaxation time, we see more interaction among the beads irrespective of their chemical nature and hence average distance between any two beads is small (a compact polymer). In Fig. S4(c), the corresponding structure is an SAW of blobs. This results in a locally folded polymer as reflected in the Fig. S4(c) (also see Fig. 4(b)).

Movie S1 (separate file): In this video we show the dynamics of a di-block copolymer of length 1024, with solvo-phillic and solvo-phobic segments of length 16, as the segments are switched from phobic/philic to philic/phobic and vice versa in a switching time of T_l . The switching time is varied from the fast switching ($T_l = 5$) to the case of the passive polymer ($T_l = \infty$). See main text for details of the model.

References

- [1] David B. Brückner, Hongtao Chen, Lev Barinov, Benjamin Zoller, and Thomas Gregor. Stochastic motion and transcriptional dynamics of pairs of distal dna loci on a compacted chromosome. *Science*, 380(6652):1357–1362, 2023.
- [2] Christopher R. Brown, Changhui Mao, Elena Falkovskaia, Melissa S. Jurica, and Hinrich Boeger. Linking Stochastic Fluctuations in Chromatin Structure and Gene Expression. *PLoS biology*, 11(8):1–15, 2013.